Appl Microbiol Biotechnol (2014) 98:739–748
DOI 10.1007/s00253-013-5159-4

Evolution of histamine oxidase activity for biotechnological applications

Elena Rosini · Fabio Tonin · Natalia Vasylieva · Stephane Marinesco · Loredano Pollegioni

Received: 29 May 2013 / Revised: 26 July 2013 / Accepted: 29 July 2013 / Published online: 31 August 2013

Abstract Histamine is present to various degrees in many foods, and concentrations in fish samples are considered a good indicator of freshness and hygienic food quality. Seeking for innovative methods to quantify histamine in foods, we used a synthetic gene designed on the sequence of histamine oxidase from *Arthrobacter crystallopoietes* (HOD) as the starting point in this study to develop a biosensor. HOD was expressed in *Escherichia coli* cells with a yield of ~7 mg protein/L of fermentation broth. Recombinant wild-type HOD oxidized histamine and tyramine whereas it was inactive toward putrescine and cadaverine (two amines present in fish samples). The putative residues involved in substrate binding were identified by an in silico docking procedure based on a model of the structure of HOD: site-saturation mutagenesis was performed on 8 positions. The most significant changes in kinetic properties were observed for the P143M HOD: this variant showed higher histamine affinity and lower substrate inhibition by tyramine than wild-type enzyme. Biosensor prototypes were produced using both the wild-type and the P143M variant HOD. These biosensors showed a good sensitivity and selectivity with respect to biogenic amines present in food specimens. Accordingly, the HOD-based biosensor was successfully used to assess histamine in fish samples, yielding values in good agreement with those obtained by HPLC analyses but in a few seconds and at a significantly lower cost per analysis.

Keywords Histamine · Amine oxidase · Biocatalysis · Biosensor · Recombinant protein

Introduction

Histamine and other biogenic amines are present to varying degrees in many foods, and their presence increases with maturation (Bodmer et al. 1999). In order for biogenic amines to form in food, free amino acids must be available, decarboxylase-positive microorganisms present, and conditions given that allow bacterial growth and decarboxylase activity. In particular, histidine is generated from autolytic or bacterial processes (Kung et al. 2012). Accordingly, high concentrations of histamine are found mainly in products of microbial fermentation, such as aged cheese, wine, and processed meat, see (Maintz and Novak 2007). Histamine concentration is considered a good indicator of fish freshness and of hygienic food quality, too; it is also known as the causative factor in scombroid poisoning, an allergy-like food poisoning (Arnold and Brown 1978). An upper limit of 200 mg histamine/kg in foods and of 2 mg histamine/L in alcoholic beverages has been suggested (Maintz and Novak 2007). Histamine accumulation may cause numerous symptoms, mimicking an allergic reaction: approximately 1 % of the population shows histamine intolerance, and 80 % of those individuals are middle aged (Komericki et al. 2011). High-performance liquid chromatography (HPLC) and also immunoenzymatic methods have largely been used to determine levels of histamine, but these

Electronic supplementary material The online version of this article (doi:10.1007/s00253-013-5159-4) contains supplementary material, which is available to authorized users.

E. Rosini · F. Tonin · L. Pollegioni (✉)
Dipartimento di Biotecnologie e Scienze della Vita, Università degli studi dell'Insubria, via J.H. Dunant 3, 21100 Varese, Italy
e-mail: loredano.pollegioni@uninsubria.it

E. Rosini · L. Pollegioni
The Protein Factory, Centro Interuniversitario di Biotecnologie Proteiche, Università degli Studi dell'Insubria, Politecnico di Milano, ICRM CNR, Milano, Italy

N. Vasylieva · S. Marinesco
Lyon Neuroscience Research Center, Team Waking, INSERM U1028; CNRS UMR5292, Lyon F-69000, France

S. Marinesco
Plate-forme technologique AniRA-Neurochem, University Lyon 1, Lyon F-69000, France

assays are time-consuming, complicated, and expensive. Seeking for alternative analytical methods, enzymatic assays based on histamine-oxidizing enzymes have been proposed.

In the past years, several groups tried to couple the enzymatic reactions on amines or amino acids with electrochemical sensors in order to obtain simple and reproducible biosensors. The biosensor procedure has certain advantages, such as low cost, short analysis time, and simplicity of use such that it can be performed outside of a scientific laboratory. As the most notable example, a commercial TPQ-containing diamine oxidase from porcine kidney (DAO, EC 1.4.3.6, 0.18 U/mg protein) was recently employed to develop a biosensor for amines using a screen-printed carbon electrode (Alonso-Lomillo et al. 2010). The main limitations of this costly enzyme were the isolation from the natural source and the broad substrate specificity, which does not discriminate between different important amines. As the first step towards engineering the substrate specificity and kinetic efficiency of mammalian DAO, the enzyme was successfully overexpressed in *Escherichia coli* cells and purified (Rosini et al. 2012). Unfortunately, the recombinant DAO was poorly active (specific activity of ≈1 mU/mg protein on histamine) because it was largely produced in an immature quinone form.

As an alternative, histamine oxidase (EC 1.4.3.6) has been proposed: it catalyzes the oxidation of histamine to imidazole acetaldehyde, ammonia, and hydrogen peroxide (Eq. 1):

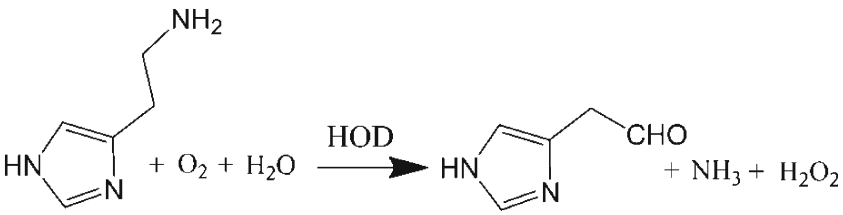

The enzyme from *Arthrobacter crystallopoietes* KAIT-B-007 (HOD) is a good candidate for this application because of its thermostability and substrate specificity (Sekiguchi et al. 2004).

In this study, we used a synthetic gene (named *hod*) designed on the basis of the primary sequence of histamine oxidase from *A. crystallopoietes* (Sekiguchi et al. 2004) to produce an enzyme active on histamine and with the properties required for a biosensor application. This goal was achieved by using a combination of protein expression optimization, molecular modeling, and site-saturation mutagenesis approaches: a recombinant, evolved HOD was generated to develop a pilot biosensor to rapidly and inexpensively quantify the amount of histamine in foods.

Materials and methods

Design and cloning of cDNA encoding for histamine oxidase

The synthetic cDNA encoding for the histamine oxidase from *A. crystallopoietes* (*hod*) was designed by in silico back translation of the amino acid sequence reported in the database (GenBank accession no. BAE48148.1). In order to facilitate the subcloning into the pET24b(+) plasmid (carrying the resistance to kanamycin, Novagen) and into the pCold I DNA plasmid (carrying the resistance to ampicillin, TaKaRa), sequences corresponding to *Nde*I (CATATG) and *Xho*I (CTCGAG) restriction sites were added at the 5′- and 3′-ends of the cDNA, respectively. Synthetic cDNA was produced by GeneArt (Life Technologies), after optimizing the coding nucleotide sequence for expression in *E. coli*. The *hod* cDNA (GenBank accession no. KF055450.1) was inserted in the pET24b(+) or pColdI vectors using the *Nde*I and *Xho*I sites, giving a 7.4-kb (pET24-HOD) or a 6.6-kb (pColdI-HOD) construct. By using the two cloning-site strategy, six codons (encoding for six additional histidines) were added to the 3′-end or at 5′-end of the *hod* gene, respectively.

Strain and growth conditions

For protein expression, plasmids containing *hod* cDNA were transferred to the *E. coli* hosts BL21(DE3), BL21(DE3)pLysS (resistant to chloramphenicol, 34 μg/mL final concentration), BL21(DE3)Star, and Origami2(DE3) (resistant to tetracycline, 12.5 μg/mL final concentration). Starter cultures were prepared from a single recombinant *E. coli* colony in LB medium containing appropriate antibiotics, under vigorous shaking at 37 °C. These cultures were diluted to a starting OD_{600nm} of 0.1 in the production media and then incubated at 37 °C on a rotator shaker at 200 rpm until protein expression was induced by adding 1 mM IPTG. The following media were used (Volontè et al. 2008): Luria-Bertani (LB, 10 g/L bacto-tryptone, 5 g/L yeast extract, 5 g/L NaCl); Terrific Broth (TB, 12 g/L bacto-tryptone, 24 g/L yeast extract, 8 mL/L glycerol, 2.2 g/L KH_2PO_4, and 9.4 g/L K_2HPO_4, corresponding to 70 mM total phosphate concentration); Super Broth (SB, 32 g/L bacto-tryptone, 20 g/L yeast extract, and 5 g/L

NaCl); and M9 minimal medium (0.5 g/L NaCl, 1 g/L NH_4Cl, 3 g/L KH_2PO_4, and 6.78 g/L Na_2HPO_4, corresponding to 68 mM total phosphate concentration, 2 mM $MgSO_4$, 0.1 mM $CaCl_2$, and 10 g/L glucose). All optimization studies were carried out in 300-mL baffled Erlenmeyer flasks containing 50 mL of liquid media. After inducing protein synthesis with IPTG, the cells were incubated at different temperatures with shaking (200 rpm) and then harvested at different times by centrifugation at 8,000×*g* for 10 min at 4 °C. For HOD chaperone coexpression, cells transformed with pET24-HOD and pKJE7 or pG-Tf2 (carrying the resistance to chloramphenicol, TaKaRa) were grown in LB medium containing L-arabinose (1 mg/mL) or tetracycline (2 ng/mL) to induce the chaperone expression, respectively (see Supplementary Material).

HOD purification and activity measurements

For protein purification trials, the cells transformed with pColdI-HOD were grown in 2-L Erlenmeyer flasks containing 500 mL of SB medium to which 10 g/L NaCl was added (SB3 medium). HOD expression was induced by adding 1 mM IPTG at the stationary phase and cells were harvested after 18 h of growth at 15 °C; cells were stored at −20 °C. Cell pellets were resuspended in lysis buffer (50 mM sodium phosphate buffer, pH 7.2, 500 mM NaCl, 1 mM pepstatine, and 10 μg/mL DNAse) and sonicated (5 cycles of 30 s each, with a 30-s interval on ice). The insoluble fraction of the lysate was removed by centrifugation at 39,000×*g* for 1 h at 4 °C. The total protein concentration in the crude extract was quantified by applying the biuret method. Crude extract was loaded onto a HiTrap chelating affinity column (GE Healthcare) that was loaded with metal ions (1 mL of 100 mM $NiCl_2$) and equilibrated with 50 mM sodium phosphate, pH 7.2, containing 500 mM NaCl (Fantinato et al. 2001). The column was washed with this buffer until the absorbance value at 280 nm was that of the buffer; the bound protein was eluted with the same buffer containing 150 mM imidazole.

Substrate specificity of HOD was investigated by spectrophotometrically determining the hydrogen peroxide produced by the enzyme reaction on different compounds. This assay was performed using a microtiter plate; each well contained 200 μL of different amines (0.1, 1, or 10 mM, final concentrations), 0.3 mg/mL *o*-dianisidine, and 1 unit/mL horseradish peroxidase in 100 mM potassium phosphate buffer, pH 7.2 at 37 °C. The product of this enzymatic reaction has an extinction coefficient of 13.4 mM^{-1} cm^{-1} at 450 nm: the increase in absorbance was followed by using a Sunrise plate reader (Tecan).

HOD activity was assayed by employing the same spectrophotometric method and 1 mM histamine. Each measurement was performed by recording the absorbance at 450 nm with a Jasco V-560 spectrophotometer, using cuvettes with a 1-cm optical path. The time course of the absorbance change was recorded at 37 °C for up to 10 min. One HOD unit is defined as the amount of enzyme that converts 1 μmol of substrate/min at 37 °C. Kinetic parameters were determined using a fixed amount of enzyme and different amine concentrations. The effect of temperature was investigated by measuring the enzymatic activity on protein samples at different temperatures (15–85 °C temperature range).

Circular dichroism spectra were recorded at 15 °C using a Jasco J-810 spectropolarimeter and analyzed by means of Jasco software (Caldinelli et al. 2005). The cell path length was 1 cm for measurements above 250 nm and 0.1 cm for measurements in the 190- to 250-nm region. Temperature-ramp experiment was performed in the 20–90 °C range by using a software-driven, Peltier-based temperature controller that allowed a temperature gradient of 0.5 °C/min. CD signal was recorded at 230 nm using an HOD sample at 0.2 mg protein/mL.

SDS-PAGE electrophoresis and Western blot analysis

Proteins from total, soluble, or insoluble cell fractions were separated by SDS-PAGE. For total cell extracts and insoluble fractions after cell disruption, pellets were directly resuspended in an appropriate volume of Laemmli sample buffer. For Western blot analysis, proteins were transferred electrophoretically onto a nitrocellulose membrane and HOD was probed through binding to anti-His-tag mouse monoclonal antibodies (His-probe, Santa Cruz Biotechnology) followed by goat anti-mouse IgG peroxidase-conjugated antibodies as secondary antibody (Santa Cruz Biotechnology) and detected by a chemiluminescence method (ECL plus Western Blotting Detection System, GE Healthcare). His-tagged D-amino acid oxidase was used as positive control (Sacchi et al. 2004).

Site-saturation mutagenesis and screening for evolved HOD variants

Site-saturation mutagenesis was carried out at different amino acid positions by using the QuikChange site-directed mutagenesis kit (Stratagene); the *hod* cDNA was subcloned into the pColdI as template and a set of degenerated synthetic oligonucleotides employed (Pollegioni et al. 2005). The template DNA was eliminated by enzymatic digestion with the *Dpn*I restriction enzyme, specific for methylated DNA; the PCR products were used to transform JM109 *E. coli* cells. Subsequently, the recombinant plasmids were transferred to BL21(DE3)Star *E. coli* cells, and these clones were used for the screening procedure. The introduction of the mutations was confirmed by automated DNA sequencing.

The mutant libraries obtained from site-saturation mutagenesis were screened by means of a rapid colorimetric assay based on the determination of hydrogen peroxide and by means of an automated liquid-handler system (epMotion 5075, Eppendorf). To a saturated *E. coli* culture (1 mL, growth in DeepWell plate, Eppendorf) 1 mM IPTG and 25 g/L NaCl

were added and the culture was then incubated at 15 °C for 18 h. The culture was centrifuged at 4,000×*g* for 2 min, and the cell pellet was resuspended with 300 μL of 50 mM sodium phosphate and 0.5 M NaCl, pH 7.2. Cell lysis was performed by adding 50 μL of 1 N NaOH and was subsequently neutralized with 50 μL of 1 M KH_2PO_4. The crude extracts were centrifuged at 4,000×*g* for 40 min and then 175 μL of the supernatant was transferred to two wells of a 96-well Elisa plate. The activity was assayed on the crude extract by adding 50 μL of substrate solution (50 mM histamine, pH 7.2, 3.2 mg/mL *o*-dianisidine, and 0.1 U/mL horseradish peroxidase in 100 mM potassium phosphate buffer, pH 7.2) and incubating the plates at 25 °C for 18 h. After the incubation, the absorbance at 440 nm was measured by a microtiter plate reader (Sunrise, Tecan) and compared with cultures expressing the wild-type HOD and untransformed cells as controls. The HOD variants that outperformed the control were selected and used for sequencing, further analysis, and biochemical characterization.

Molecular modeling and docking analysis

Sequence alignments were generated by T-coffee software (Notredame et al. 2000). The 3D model of HOD was built using the Swiss-model server (Guex and Peitsch 1997; Schwede et al. 2003), employing the entire structure of amine oxidase from *A. globiformis* (PDB code 1W6G, 646 residues, 55 % of sequence identity) as template (Juda et al. 2001). The HOD model was validated using What_Check (Hooft et al. 1996) and Verify_3D (Luthy et al. 1992) servers. The three-dimensional structure of the substrate histamine was generated using the PRODRG2 server (Schuttelkopf and van Aalten 2004). Automated ligand docking was performed by Autodock Vina, a package based on a Montecarlo simulated annealing approach (Trott and Olson 2010; Golden et al. 2013) with a square grid box constructed to cover the region targeted for active site and with the default setting of exaustiveness.

Histamine detection by HPLC

HPLC analyses were performed on a Merck Hitachi apparatus equipped with a L-6200 pump and an L-4200 UV–Vis detector and fitted with a Phenomenex Luna C18(2) column (length/internal diameter 250/4.6 mm, pore size 5 μm) under the following conditions: eluent 50 mM acetate buffer, pH 5.2/CH_3OH (90/10 vol/vol), flux 0.8 mL/min, detection at 340 nm. Solvents were of analytical grade. The different amine solutions and the fish samples were derivatized with the OPA-NAC reagent as described in (Zhao and Bada 1995). Five grams of tuna (purchased at a fish market) were cut into small pieces by scissors and 15 mL of 5 % trichloroacetic acid was added. The sample was then homogenized and sonicated (5 cycles of 30 s each, with a 30-s interval on ice); the insoluble fraction was removed by centrifugation at 39,000×*g* for 20 min at 4 °C. The homogenate was then transferred to a 100-mL volumetric flask and the jar rinsed seven times with 15 mL of the extracting solvent (diethyl ether). The supernatant was filtered using a 0.2-μm filter membrane, diluted as required, and treated as reported before.

Histamine detection by a biosensor

Platinum microelectrodes were prepared as reported in (Vasylieva et al. 2011). The enzyme layer was deposited by dipping the Pt tip of the electrode in the enzyme solution at a HOD concentration of 60 mg/mL, 30 mg/mL bovine serum albumin, and 10- to 40-mg/mL poly(ethylene glycol)diglycidyl ether (PEGDE) for cross-linking (in 10 mM phosphate-buffered saline, pH 7.4). To achieve selective detection, all microelectrodes were coated with a layer of poly-*m*-phenylenediamine (PPD). All measurements were performed in 10 mM phosphate-buffered saline under a constant potential of 500 mV versus an Ag/AgCl reference electrode.

Results

Purification and characterization of recombinant HOD

The synthetic cDNA encoding for histamine oxidase from *A. crystallopoietes* (Sekiguchi et al. 2004), whose codon usage was optimized for protein expression in *E. coli* (GenBank accession no. KF055450.1), was cloned in pColdI plasmid using the *Nde*I and *Xho*I sites yielding the pColdI-HOD expression plasmid. The expression of an active HOD in *E. coli* was demonstrated by selection on a mineral medium agar plate containing histamine as the only carbon source. As shown in Fig. 1, only the

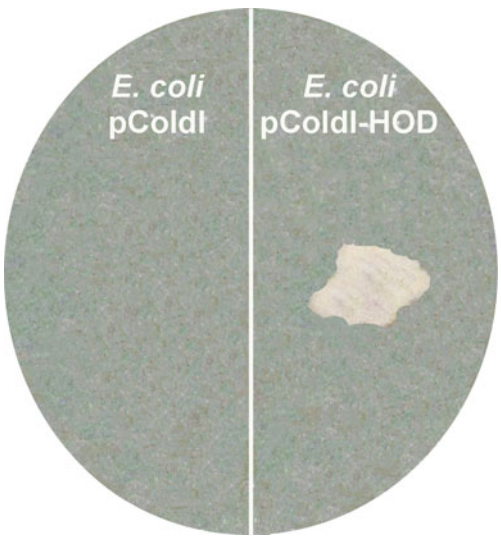

Fig. 1 *E. coli* BL21(DE3)Star colonies transformed with pColdI or pColdI-HOD plasmids were grown on a M9 mineral medium containing histamine as the only carbon source

E. coli (DE3)Star cell clones expressing HOD (induced with 1 mM IPTG and 25 g/L NaCl and incubated at 15 °C) grew on selective plates.

Best conditions for laboratory-scale production of HOD (see Fig. S1 and S2 in Supplementary Material) were identified as the use of *E. coli* BL21(DE3)Star cells transformed with the pColdI-HOD plasmid, grown at 37 °C in SB3 medium, added at the stationary phase of 25 g/L NaCl and 1 mM IPTG, and collected after 24 h of incubation at 15 °C: about 7 mg/L of soluble HOD was obtained.

Recombinant HOD expressed using pColdI-HOD plasmid contains a His-tag at the C-terminus; thus, it was purified by using HiTrap chelating affinity chromatography. By employing a single chromatographic step followed by 1 week of incubation at 4 °C (see below), recombinant HOD was isolated as a single band at ≈75 kDa, with a >80 % yield and to a >90 % purity (as judged by SDS-PAGE, see Fig. 2): ≈3 mg of purified HOD/L fermentation broth was thus obtained. Intriguingly, at the end of the purification procedure the enzyme sample showed two close bands in SDS-PAGE analysis (at ≈81 and 75 kDa, see Fig. S3 left in the Supplementary Material), both recognized by anti-His-tag antibody. Only the lighter form was present after 1 week of incubation: it might originate from cleavage of approx. 60 residues at the N-terminal end of HOD (Fig. S3 right in the Supplementary Material).

The specific activity of freshly purified HOD on histamine as substrate is 0.05 U/mg protein. A significant increase in enzymatic activity was observed following the incubation at 4 °C for 1 week (up to 0.2 U/mg protein) although the content in secondary and tertiary structure was not affected, as made evident by comparing the circular dichroism spectra (Fig. S4 in the Supplementary Material). The purified HOD completely lost the activity when stored at −20 °C. The addition of 1 mM $CuSO_4$, 1 mM 2-mercaptoethanol, 10 % DMSO, or 0.1 % SDS did not affect the enzymatic activity (data not shown).

The activity of pure HOD was assayed on L-histidine (precursor of histamine) and several amines that could be present in foods (benzylamine, histamine, tyramine, putrescine, and cadaverine) by the peroxidase/*o*-dianisidine spectrophotometric assay at three different substrate concentrations (0.1, 1, 10 mM) and using a microtiter plate. The results only confirmed HOD activity on histamine and tyramine (see Fig. 3a), as reported in Sekiguchi et al. (2004). The apparent kinetic parameters for these two amines are reported in Table 1: a two-fold higher enzymatic activity was observed on histamine. A substrate-inhibition effect was observed for the wild-type HOD with histamine and, in particular, tyramine (K_i=0.3 mM, Table 1). Indeed, HOD was also active on two monoamine neurotransmitters such as dopamine and serotonin: the V_{max}/K_m ratio was five- to seven-fold lower than with histamine as substrate.

Protein engineering of HOD

Since the three-dimensional structure of *A. crystallopoietes* HOD is unknown, a model of the protein was built by comparative modeling using the Swiss-model facility (Fig. 4a) (Guex and Peitsch 1997; Schwede et al. 2003). Amine oxidase from *A. globiformis* (PDB code 1W6G) was chosen as template because of the high sequence identity (55 %) with HOD (Juda et al. 2001). The binding mode of the substrate histamine in the model of the HOD active site (shown in Fig. 4b) was then simulated using Autodock Vina software (Trott and Olson 2010; Golden et al. 2013). In the best solutions (the ones possessing the lowest energy), histamine perfectly matches the active site of HOD (Fig. 4b) and is bound in a similar orientation as the inhibitor berenil in the active site of human DAO (McGrath et al. 2009): the amidinium group, deeply inserted into active site, interacts with the two carboxylate oxygen atoms of the putative catalytic base Asp304 and the substrate phenyl ring with Tyr308 (corresponding to Asp373 and Tyr371, respectively, in human DAO); for the latter enzyme, however, the preference for histamine was explained by the electrostatic interaction of its imidazole

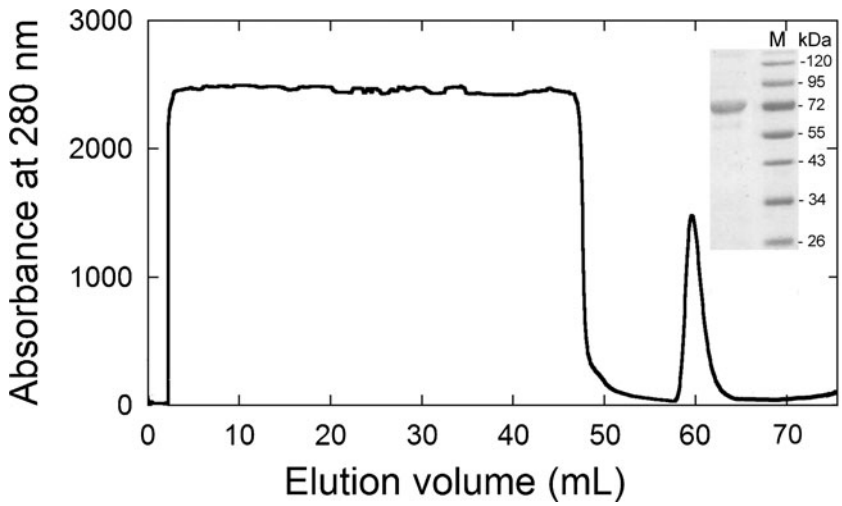

Fig. 2 Elution profile of HiTrap chelating chromatography of the recombinant HOD purification. *Insert* SDS-PAGE analysis of eluted fraction. Gel was stained with Coomassie blue. (*M*) Molecular weight marker proteins

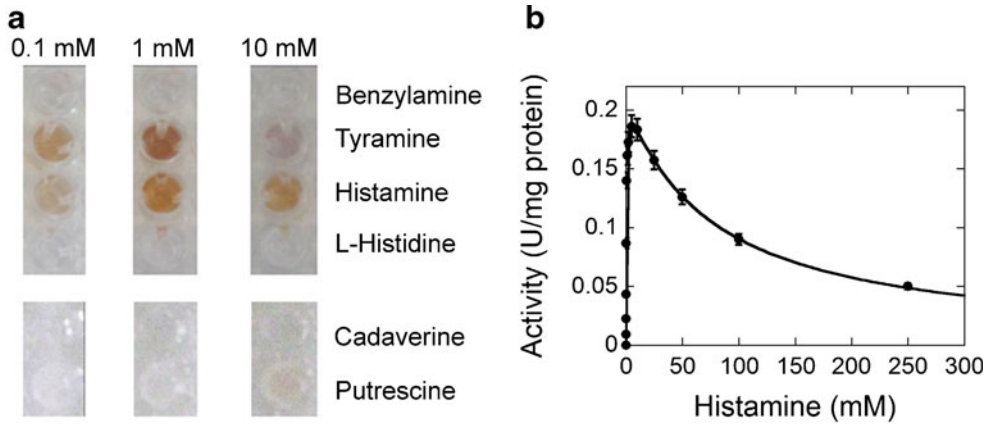

Fig. 3 **a** Activity assay of pure HOD wild-type on several amines and L-histidine on a microtiter plate. **b** Dependence of the activity values for the reaction of wild-type HOD from the concentration of histamine. The data points (average of at least three single experiments) are from fits based on the modification of a classical Michaelis–Menten equation for a substrate-inhibition effect. The colorimetric assay was based on the spectrophotometric determination of the hydrogen peroxide produced by the HOD reaction in the presence of different substrate concentrations, at 37 °C

nitrogen with Asp186. In addition to the tyrosine residue reported above, the docking model of the HOD-histamine complex identified further protein residues that could modulate the interaction with the substrate: Phe112, Asp117, Pro143, Leu144, Leu160, Arg312, and Gly386 (Fig. 4b).

On the basis of the in silico analysis, site-saturation mutagenesis was independently performed at positions 112, 117, 143, 144, 160, 308, 312, and 386 using the QuikChange kit and the wild-type *hod* cDNA as template. The activity of HOD variants on histamine as substrate was screened on a microtiter plate using the coupled peroxidase/*o*-dianisidine spectrophotometric method (that assays H_2O_2 produced by HOD) and an automated liquid-handler system. For each position, 200–250 clones were screened, a number that gives a probability of 96 % that every single amino acid is introduced (Pollegioni et al. 2005). The clones most active on histamine as identified through the screening procedure were isolated and the substitutions were identified by automatic DNA sequencing. Here, 13 HOD variants were expressed in *E. coli* BL21(DE3)Star cells and purified by HiTrap chelating chromatography (>90 % purity). All of the variants show an expression yield similar to that of the wild-type HOD (in terms of purified protein/liter of fermentation broth, see Table 1), the only exception being the ones at positions 308 and 312, whose production level was up to six-fold lower.

As shown in Table 1, among the HOD variants obtained by site-saturation mutagenesis and purified to homogeneity, the P143M HOD was identified because of a three-fold increase in histamine affinity and a 1.5-fold increase in the specificity constant (the V_{max}/K_m ratio between histamine and tyramine) compared to wild-type HOD. The G386A variant possessed similar kinetic properties on both substrates, with an increased

Table 1 Level of expression in *E. coli* BL21(DE3)Star cells and kinetic properties of wild-type and variants of HOD

	Expression level (mg protein/L culture)[a]	Histamine				Tyramine			
		V_{max} (U/mg)	K_m (mM)	V_{max}/K_m	K_i (mM)	V_{max} (U/mg)	K_m (mM)	V_{max}/K_m	K_i (mM)
Wild-type	3.10	0.20±0.005	0.30±0.03	0.70	75±9.8	0.10±0.02	0.05±0.01	2.0	0.3±0.09
F112G	3.05	0.01±0.001	0.73±0.15	0.01	38±4.7	b.d.			
F112L	2.10	0.03±0.001	1.06±0.22	0.02	77±11.1	b.d.			
F112T	3.40	0.12±0.05	0.64±0.21	0.20	97±21.3	0.04±0.002	0.14±0.04	0.3	4.4±0.5
D117I	1.50	0.06±0.005	0.63±0.19	0.10	105±20.0	b.d.			
D117L	3.50	0.12±0.04	0.64±0.23	0.20	27±4.9	b.d.			
D117V	2.50	0.03±0.002	0.43±0.07	0.06	32±5.9	0.04±0.002	0.07±0.01	0.5	5.0±0.8
P143M	3.00	0.10±0.003	0.10±0.02	1.00	64±8.7	0.10±0.004	0.05±0.005	2.0	7.3±1.3
L144A	2.00	0.02±0.001	4.2±0.4	0.005	/	0.02±0.001	0.06±0.005	0.03	/
G386A	2.40	0.07±0.001	0.27±0.02	0.03	84±7.1	0.07±0.002	0.06±0.01	1.2	3.1±0.4

Activity was assayed with the spectrophotometric method at 37 °C and pH 7.2

b.d. below detection

[a] Expression level of further HOD variants (mg protein/L culture): Y308A: 0.45; Y308S: 0.60; R312A: 0.45; R312G: 0.80

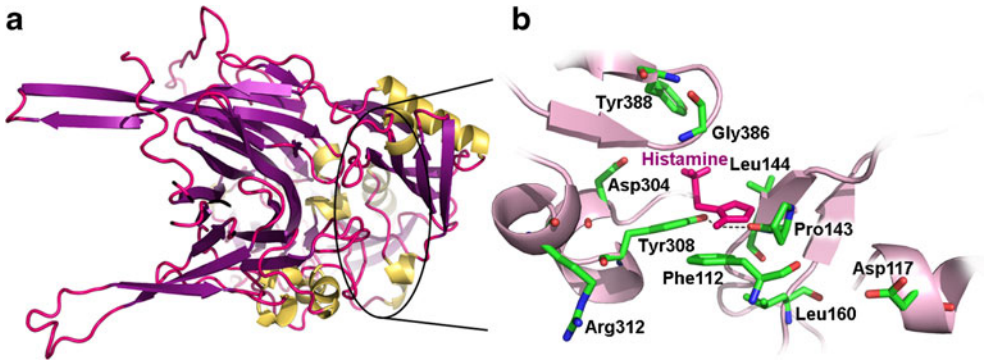

Fig. 4 **a** Ribbon representation of a three-dimensional model of HOD (helices are depicted in *yellow*, sheets in *purple*, and coils in *pink*). **b** Results of histamine binding to the HOD active site by using the Autodock Vina program. The substrate conformation possessing the lowest docked energy is depicted in *pink*. The hydrogen bonds are marked as *dotted lines*

K_i value on tyramine (up to ten-fold) in comparison to wild-type HOD. Comparison of the kinetic parameters of wild-type and variants of HOD at positions 112 and 117 indicates that the decrease in kinetic efficiency on histamine and tyramine was mainly caused by a dramatic drop in V_{max} (up to 20-fold for the F112G enzyme, the only exception being F112T HOD), while for both substrates the K_m parameters were altered to a lesser extent (less than three-fold), see Table 1. Notably, the P143M variant was inhibited by tyramine at higher concentrations than wild-type HOD and showed a 70-fold lower V_{max}/K_m ratio for serotonin as compared to histamine (while the activity on dopamine was unchanged).

Experiments on temperature dependence of the enzymatic activity showed that HOD activity increased with temperature up to 85 °C (≈ 1.6-fold in comparison with the activity determined at 37 °C, see Fig. S5 in the Supplementary Material). Interestingly, the P143M HOD variant is comparatively more active at low temperature than the wild-type counterpart (in particular, at 15 °C it maintained ≈50 % of the activity determined at 37 °C); furthermore, it fully retained the activity after treatment at 37 °C for 24 h or at 25 °C for 1 week (not shown). Temperature-ramp experiments following the change in the circular dichroism signal at 230 nm showed a higher melting temperature for the P143M variant than for the wild-type HOD (66.5 °C and 60.8 °C, respectively).

HOD-based biosensor and analysis of histamine in fish samples

A biosensor based on a platinum microelectrode with a sensing tip of 25 μm in diameter and 100 μm in length was employed (Pernot et al. 2008; Vasylieva et al. 2011). The platinum tip was then covered by a layer of PPD and a membrane of enzyme immobilized with PEGDE (Vasylieva et al. 2011). Experiments performed on biosensors prepared with wild-type HOD immobilized with PEGDE showed a response to histamine of 12.7±7.0 pA/μM (n=8), with an apparent K_m value of 104±17 μM (Table 2, n=6). The time to reach 10 to 90 % of the biosensor response was 1.5 s. The amperometric response was linear with a histamine concentration of up to about 20 μM. The selectivity of the biosensors was investigated in the presence of different, potentially interfering molecules (n=8): putrescine and cadaverine (0.1 mM final concentration) generated a negligible response (1±0.7 % of the histamine response for putrescine, not detectable for cadaverine). When used in the biosensor, the P143M variant showed a sensitivity of 9.8±6 μM, which is not significantly different from that obtained with the wild-type HOD (n=8, p=0.28), and a K_m of 45±6 μM for histamine. This lower K_m value than with wild-type HOD was in good agreement with the kinetic parameters determined for the free enzyme form (Tables 1 and 2). In addition, the selectivity of the P143M HOD-based biosensors showed a 0.7±0.2 % response to putrescine (expressed as % of the histamine response), and cadaverine was not detectable. The detection limit of the biosensor was 15 nM (determined as 3× rms noise). Both types of biosensors responded to amine neurotransmitters: 163±90 % to dopamine and 19±3 % to serotonin.

The simultaneous resolution and quantification of biogenic amines can be performed by HPLC separation and an OPA-NAC derivatization procedure; histamine, histidine, tyramine, putrescine, and cadaverine were resolved on the Luna C18 column in ≈40 min by HPLC. The best result was obtained using an acetate buffer at pH 5.2: Fig. S6a in the Supplementary Material reports the calibration between the area responses to the corresponding histamine amounts that were injected. The detection limit for histamine is 15 ng, corresponding to 5 mg of histamine/kg fish product; this value is significantly lower than

Table 2 Response of the biosensor developed using wild-type or P143M HOD on histamine

HOD variant	K_m (μM)	Response (pA/μM)
Wild-type	104±17	12.7±7.0
P143M	45±6	9.8±1.6

the regulation limit for histamine in fish products, corresponding to 200 mg histamine/kg fish product (Maintz and Novak 2007). The histamine content determined for a fresh tuna sample and the same conserved at room temperature for 1 week at 25 °C showed an increase from 35 to 450 mg histamine/kg fish. Interestingly, adding HOD to the tuna sample stored at 25 °C fully eliminated the peak corresponding to histamine (20 mU of wild-type HOD added to 0.75 mg of histamine for 10 min at 25 °C, Fig. S6b in the Supplementary Material). Furthermore, the same increase in histamine concentration as detected by classical HPLC analysis was also obtained by the HOD-based biosensor (i.e., a 1.4-fold increase in histamine concentration after 5 h at 25 °C).

Discussion

Biochemical properties

In this work, a thermostable HOD was expressed and purified from *E. coli* cells. The enzyme, produced with an His-tag at the C-terminus, was isolated by a single chromatographic step with an overall yield of ≈3 mg protein/L of fermentation broth: this figure is significantly higher than the yield of recombinant *A. globiformis* HOD in *E. coli* previously reported (i.e., 1.2 mg/L of fermentation broth) (Iwaki et al. 2002). Wild-type HOD shows activity on histamine and tyramine (Table 1), whereas it is inactive toward putrescine and cadaverine (two amines present in biological samples, for example, in fish). The specific activity of recombinant HOD purified in this work is almost equal to ten-fold lower than the value reported by (Ito et al. 2009): a rationale for this is not straightforward, even though we have to mention that the two assays differed in pH, ionic strength and dye used. Diamine oxidases show classical inhibition by substrate, in that their activity decreases at high substrate concentration (Elmore et al. 2002). Such an inhibition was observed also for the wild-type HOD with histamine and, in particular, tyramine (K_i=0.3 mM, Table 1) as substrate: this represents a main drawback in the use of the enzyme as an analytical tool. Interestingly, the P143M variant (see below) was inhibited at higher concentrations than wild-type HOD by tyramine. Indeed, both recombinant HOD forms show optimal activity at high temperature and good storage stability (fully retaining the enzymatic activity after 1 week at 25 °C).

Protein engineering

We built a model of the tertiary structure of HOD that was based on the 3D structure of *A. globiformis* amine oxidase (Fig. 4a); by using this model and an in silico docking procedure we could identify the putative residues involved in substrate binding (Fig. 4b). In order to alter the kinetic properties of HOD and gain deeper insight into its structure–function relationships, site-saturation mutagenesis was performed on eight positions. Screening of the ensuing libraries on histamine showed that substitution of Tyr308 or Arg312 was associated with abolition of enzymatic activity in all cases, this providing strong evidence for proposing a main role for these residues in substrate binding (the previous) and in keeping the overall active site arrangement (the latter residue). Variants at positions 112, 117, 144, and 386 showed a decreased kinetic efficiency on both histamine and tyramine as substrates (and no relevant variants were identified from screening of the library for position 160), see Table 1. Introduction of substitutions at positions 308 and 312 yielded HOD variants expressed at lower levels than the wild-type one (Table 1). These latter residues belong to a region with a low intrinsic propensity to structural disorder, as identified using the RONN and DisEMBL servers (Linding et al. 2003; Yang et al. 2005): an increase in disorder, as a result of introducing substitutions at such positions, should affect the solubility of the resulting variant protein.

HOD is a thermostable enzyme with a quite rigid structure: interestingly, positions 143 and 144 belong to a region with higher propensity to disorder and resulted in variants with altered kinetic properties. The P143M HOD variant shows a higher histamine affinity and a higher specificity constant than the wild-type enzyme does (see Table 1). The P143M HOD also shows lower substrate inhibition by tyramine than the wild-type enzyme, an effect that was completely abrogated for the L144A variant on both histamine and tyramine. The K_i value for histamine of HOD is higher than that observed for rat DAO, ≈70 vs. 30 mM, respectively (Elmore et al. 2002), and significantly higher than the amount of this biogenic amine in biological fluids, thus not affecting an assay based on HOD. Indeed, the P143M variant distinguishes from the wild-type HOD for a higher activity at temperature ≤30 °C and for a 6 °C higher melting temperature. All together, these results suggest an effect of the introduced substitution at position 143 on the thermal dependence of protein dynamics that in turn affects its stability and activity.

HOD-based biosensor

Histamine is not present in fresh fish while it is produced when the fish has been contaminated with microorganisms. The food industry generally favors the HPLC method for controlling fish products since it provides information on the composition of the biogenic amines. This is important as the presence of other amines in addition to histamine might intensify symptoms in the case of poisoning. When such extensive information is not required and the cost per analysis is a limiting factor, an enzymatic assay of histamine is preferred. We addressed the problem of identifying a suitable enzyme for such an application. Histamine oxidase from *A. globiformis* showed a greater affinity for tyramine than for histamine (Choi et al. 1995) and rat

diamine oxidase showed higher V_{max} on benzylamine and tyramine than on histamine (Rosini et al. 2012). Nonetheless, biosensors for histamine detection were developed using the enzymes isolated from the natural source (Iwaki et al. 2002; Wasoh et al. 2012). The capacity biosensor based on immobilized commercial DAO showed a limited linear relationship between histamine concentration and frequency (50–200 ppm range, corresponding to 0.45–1.8 mM) and required 300 s to reach the final change in dielectric properties (Wasoh et al. 2012). On the other hand, the amperometric sensor based on *A. globiformis* HOD responded to a number of bioamines in addition to histamine, thus showing a limited specificity (Iwaki et al. 2002). The problem of the limited specificity of DAO for histamine was solved using an HOD assay combined with the amperometric determination of hydrogen peroxide by a peroxidase-modified carbon electrode, which enabled detection at low operating potential (Hibi and Senda 2000). HOD from the thermophilic *A. crystallopoietes* was also proposed since it showed remarkable activity on histamine whereas was inactive toward putrescine, cadaverine, spermine, and spermidine (Sekiguchi et al. 2004). Accordingly, an efficient flow injection analysis device (lower detection limit of 1 μM) was produced using HOD immobilized with chitosan beads (Ito et al. 2009): the main limit was the elaborated device and the storage stability of the reactor.

Here, we set up a prototype for a simple biosensor based on recombinant HOD, both the wild-type and the P143M variant obtained by site-saturation mutagenesis on selected positions identified by a rational approach. The HOD-based biosensors showed a good sensitivity and selectivity with respect to biogenic amines present in a food specimen. The biosensor employing the P143M HOD variant exhibited a higher affinity for histamine than did the wild-type HOD. Furthermore, P143M HOD showed less substrate inhibition by tyramine. We should note that the cross-linking methods used to immobilize enzymes on biosensors are likely to induce a slight loss in enzyme substrate specificity (Vasylieva et al. 2013). In our hands, biosensors prepared with wild-type or P143M HOD cross-linked with PEGDE did not show any significant difference in sensitivity or in selectivity. The HOD-based biosensors were successfully employed to analyze fish samples, yielding increases in histamine values in good agreement with those obtained by HPLC analysis but in only a few seconds vs. 7 and 12 min in (Hibi and Senda 2000; Iwaki et al. 2002), and with a significant decrease in the cost per analysis. Indeed, the detection limit was 0.5 mg/100 g wet tissue, ten-fold lower than previous report (Hibi and Senda 2000).

In conclusion, the HOD-based biosensor provides an attractive method to quickly estimate histamine content in food preparations that do not contain high concentrations of dopamine or serotonin. In particular, the biosensor can efficiently detect changes in histamine concentration when the fish is decaying.

Acknowledgments This study was financially supported by Regione Lombardia "Accordi per la Cooperazione Internazionale–Progetto Istansensor: 15764, Rif. SAL-35", and by Fondo di Ateneo per la Ricerca to L. Pollegioni. SM and NV were supported by Région Rhône-Alpes COOPERA CMIRA 2012. We thank Andrea Fiorati for HPLC analyses, Gianluca Molla for docking and structural analyses, Laura Caldinelli for CD measurements and Federica Volontè and Roberta Melis for technical support. We thank the support from Consorzio Interuniversitario per le Biotecnologie CIB.

References

Alonso-Lomillo MA, Dominguez-Renedo O, Matos P, Arcos-Martinez MJ (2010) Disposable biosensors for determination of biogenic amines. Anal Chim Acta 665(1):26–31

Arnold SH, Brown WD (1978) Histamine (?) toxicity from fish products. Adv Food Res 24:113–154

Bodmer S, Imark C, Kneubuhl M (1999) Biogenic amines in foods: histamine and food processing. Inflamm Res 48(6):296–300

Caldinelli L, Iametti S, Barbiroli A, Bonomi F, Fessas D, Molla G, Pilone MS, Pollegioni L (2005) Dissecting the structural determinants of the stability of cholesterol oxidase containing covalently bound flavin. J Biol Chem 280(24):22572–22581

Choi YH, Matsuzaki R, Fukui T, Shimizu E, Yorifuji T, Sato H, Ozaki Y, Tanizawa K (1995) Copper/topa quinone-containing histamine oxidase from *Arthrobacter globiformis*. Molecular cloning and sequencing, overproduction of precursor enzyme, and generation of topa quinone cofactor. J Biol Chem 270(9):4712–4720

Elmore BO, Bollinger JA, Dooley DM (2002) Human kidney diamine oxidase: heterologous expression, purification, and characterization. J Biol Inorg Chem 7(6):565–579

Fantinato S, Pollegioni L, Pilone MS (2001) Engineering, expression and purification of a His-tagged chimeric D-amino acid oxidase from *Rhodotorula gracilis*. Enzym Microb Technol 29(6–7):407–412

Golden E, Paterson R, Tie WJ, Anandan A, Flematti G, Molla G, Rosini E, Pollegioni L, Vrielink A (2013) Structure of a class III engineered cephalosporin acylase: comparisons with class I acylase and implications for differences in substrate specificity and catalytic activity. Biochem J 451(2):217–226

Guex N, Peitsch MC (1997) SWISS-MODEL and the Swiss-PdbViewer: an environment for comparative protein modeling. Electrophoresis 18(15):2714–2723

Hibi T, Senda M (2000) Enzymatic assay of histamine by amperometric detection of H_2O_2 with a peroxidase-based sensor. Biosci Biotechnol Biochem 64(9):1963–1966

Hooft RW, Vriend G, Sander C, Abola EE (1996) Errors in protein structures. Nature 381(6580):272

Ito T, Hiroi T, Amaya T, Kaneko S, Araki M, Ohsawa T, Yamamura A, Matsumoto K (2009) Preliminary study of a microbeads based histamine detection for food analysis using thermostable recombinant histamine oxidase from *Arthrobacter crystallopoietes* KAIT-B-007. Talanta 77(3):1185–1190

Iwaki S, Ogasawara M, Kurita R, Niwa O, Tanizawa K, Ohashi Y, Maeyama K (2002) Real-time monitoring of histamine released from rat basophilic leukemia (RBL-2H3) cells with a histamine microsensor using recombinant histamine oxidase. Anal Biochem 304(2):236–243

Juda GA, Bollinger JA, Dooley DM (2001) Construction, overexpression, and purification of *Arthrobacter globiformis* amine oxidase-Strep-tag II fusion protein. Protein Expr Purif 22(3):455–461

Komericki P, Klein G, Reider N, Hawranek T, Strimitzer T, Lang R, Kranzelbinder B, Aberer W (2011) Histamine intolerance: lack of reproducibility of single symptoms by oral provocation with

histamine: a randomised, double-blind, placebo-controlled cross-over study. Wien Klin Wochenschr 123(1–2):15–20

Kung HF, Tsai YH, Chang SC, Hong TY (2012) Biogenic amine content, histamine-forming bacteria, and adulteration of pork in tuna sausage products. J Food Prot 75(10):1814–1822

Linding R, Jensen LJ, Diella F, Bork P, Gibson TJ, Russell RB (2003) Protein disorder prediction: implications for structural proteomics. Structure 11(11):1453–1459

Luthy R, Bowie JU, Eisenberg D (1992) Assessment of protein models with three-dimensional profiles. Nature 356(6364):83–85

Maintz L, Novak N (2007) Histamine and histamine intolerance. Am J Clin Nutr 85(5):1185–1196

McGrath AP, Hilmer KM, Collyer CA, Shepard EM, Elmore BO, Brown DE, Dooley DM, Guss JM (2009) Structure and inhibition of human diamine oxidase. Biochemistry 48(41):9810–9822

Notredame C, Higgins DG, Heringa J (2000) T-Coffee: a novel method for fast and accurate multiple sequence alignment. J Mol Biol 302(1):205–217

Pernot P, Mothet JP, Schuvailo O, Soldatkin A, Pollegioni L, Pilone M, Adeline MT, Cespuglio R, Marinesco S (2008) Characterization of a yeast D-amino acid oxidase microbiosensor for D-serine detection in the central nervous system. Anal Chem 80(5):1589–1597

Pollegioni L, Lorenzi S, Rosini E, Marcone GL, Molla G, Verga R, Cabri W, Pilone MS (2005) Evolution of an acylase active on cephalosporin C. Protein Sci 14(12):3064–3076

Rosini E, Nossa S, Valentino M, D'Arrigo P, Marinesco S, Pollegioni L (2012) Expression of rat diamine oxidase in *Escherichia coli*. J Mol Catal B Enzym 82:115–120

Sacchi S, Rosini E, Molla G, Pilone MS, Pollegioni L (2004) Modulating D-amino acid oxidase substrate specificity: production of an enzyme for analytical determination of all D-amino acids by directed evolution. Protein Eng Des Sel 17(6):517–525

Schuttelkopf AW, van Aalten DM (2004) PRODRG: a tool for high-throughput crystallography of protein–ligand complexes. Acta Crystallogr D Biol Crystallogr 60(Pt 8):1355–1363

Schwede T, Kopp J, Guex N, Peitsch MC (2003) SWISS-MODEL: an automated protein homology-modeling server. Nucleic Acids Res 31(13):3381–3385

Sekiguchi Y, Makita H, Yamamura A, Matsumoto K (2004) A thermostable histamine oxidase from *Arthrobacter crystallopoietes* KAIT-B-007. J Biosci Bioeng 97(2):104–110

Trott O, Olson AJ (2010) Software News and Update AutoDock Vina: improving the speed and accuracy of docking with a new scoring function, efficient optimization, and multithreading. J Comput Chem 31(2):455–461

Vasylieva N, Barnych B, Meiller A, Maucler C, Pollegioni L, Lin JS, Barbier D, Marinesco S (2011) Covalent enzyme immobilization by poly(ethylene glycol) diglycidyl ether (PEGDE) for microelectrode biosensor preparation. Biosens Bioelectron 26(10):3993–4000

Vasylieva N, Maucler C, Meiller A, Viscogliosi H, Lieutaud T, Barbier D, Marinesco S (2013) An immobilization method for biosensors with preserved enzyme specificity: consequences for glutamate detection in the central nervous system. Anal Chem 85:2507–2515

Volontè F, Marinelli F, Gastaldo L, Sacchi S, Pilone MS, Pollegioni L, Molla G (2008) Optimization of glutaryl-7-aminocephalosporanic acid acylase expression in *E. coli*. Protein Expr Purif 61(2):131–137

Wasoh H, Hengb LY, Abu Bakar F, Wagiran R, Salleh A, Yusof NA, Misrond N, Rahmane FHA (2012) A simple capacitive biosensor device for histamine measurement. Sens Rev 32(3):245–250

Yang ZR, Thomson R, McNeil P, Esnouf RM (2005) RONN: the bio-basis function neural network technique applied to the detection of natively disordered regions in proteins. Bioinformatics 21(16):3369–3376

Zhao M, Bada JL (1995) Determination of alpha-dialkylamino acids and their enantiomers in geological samples by high-performance liquid chromatography after derivatization with a chiral adduct of *o*-phthaldialdehyde. J Chromatogr A 690:55–63